20th International Conference on Structural Mechanics in Reactor Technology (SMiRT 20)
Espoo, Finland, August 9-14, 2009
SMiRT 20-Division-II, Paper 1864

Fatigue Crack Initiation and Crack Growth Studies for Pipes made of Carbon Steel

Punit Arora, Suneel K Gupta, P.K. Singh, Vivek Bhasin, K. K. Vaze, A.K. Ghosh and H. S. Kushwaha

Reactor Safety Division, Bhabha Atomic Research Center, Mumbai, 400085, India
e-mail: punit@barc.gov.in

Keywords: Characteristic distance, low cycle fatigue, multiaxiality, fatigue crack growth

1 ABSTRACT

Experimental studies were carried out to understand the behaviour of 8″ Sch.100 carbon steel (SA 333 Gr.6) notched pipes subjected to pure alternating bending moment using four point bend setup. The procedure as given in A-16 guide of RCC-MR for fatigue crack initiation was used to back calculate a characteristic distance (d_i) from the notch root at which the elastic plastic strain field would lead to experimentally obtained number of cycles for initiation. The 3D finite element analyses of actual notched pipes as under tested conditions were carried out to rule out approximations present in A-16 and compare d_i as obtained from FE analysis with A-16 results. Further, the fatigue crack growth curves (*a* versus *N*) obtained from actual pipe tests are in good agreement with the analytical results obtained using Paris Law.

2 INTRODUCTION

The failure of the piping components may occur well below the allowable stress limits even under normal operating conditions. This may be attributed to the presence of flaws which have either gone undetected during pre-service inspection or appeared in due course of its service. Such failures need a detailed stress/ strain analysis to guarantee the component integrity under fatigue loading. Therefore, an alternate fail-safe design philosophy such as Leak-Before-Break (LBB) which is based on fracture mechanics concepts is adopted and requires rigorous integrity assessment of piping component with postulated part through thickness flaw. It is required to be demonstrated that the unstable tearing will never occur before the crack penetrates through thickness and gives easily detectable leakage. This requires investigation on fatigue crack initiation followed by fatigue crack growth (FCG) of piping components with different postulated part through flaws for the qualification of LBB design criterion. Additionally, fatigue crack initiation and crack growth data of actual piping components will be useful for the accurate life prediction of the older Nuclear Power Plants (NPP).

In view of this, six numbers of tests were carried out by Singh et al. (2003) on 8″ Sch.100 carbon steel straight pipes having circumferential part through notch. These pipes were subjected to pure alternating bending moment using four point bend setup. The material is similar to that used in primary heat transport (PHT) piping of Indian Pressurised Heavy Water Reactor (PHWR) and conforms to the specifications SA 333 Gr. 6 of ASME section II and section III. The initial aspect ratios (2c/a) of the notches varied from 19 to 58 and the initial notch depth to thickness (a/t) ratios varied from 0.125 to 0.4. The variation of maximum remote stress was taken from $0.4\sigma_y$ to $0.7\sigma_y$ with the stress ratios (R) of 0.1 and 0.5. The Alternating Current Potential Drop (ACPD) technique was used to determine the crack initiation and growth of crack front. The crack is assumed to be initiated when it grows by 0.1 mm, this is due to the limitation in sensitivity of the instrument. The cycles to crack initiation for different tests range from 3000 to 320,000 and the cycles for crack to grow through wall fall in the range of 53000 to 869,000.

Fatigue crack initiation has been widely studied in past using notched specimens by Neuber H. (1961), Topper et al. (1969), Hoffmann and Seeger (1985) to evaluate the local stress/ strain field from the stress/ strain concentration approach whereas Molski and Glinka (1981) applied equivalent strain energy density method (ESED) to evaluate the same. This amplified local strain predicts the approximate number of cycles for crack initiation using low cycle fatigue curve. In this paper, an approximate methodology of A-16 guide

of RCC-MRR for leak before break analysis and defect assessment which is used to evaluate the local stress and strain field based on stress/ strain concentration approach, is adopted. A16 requires strain calculations to be carried out at characteristic distance from the notch root to yield initiation life. This characteristic distance (d_i) is stated to be a material specific parameter by A-16 irrespective of the load applied and notch geometrical parameters. In view of this, characteristic distances were evaluated for all the six pipes using A-16 procedure for the material which was fatigue tested. Hence, fatigue crack initiation life can be predicted if d_i is a material specific parameter. The study was further extended using finite element analysis due to geometrical limitations in A-16 procedure. Hence, the characteristic distances were evaluated from the actual state of stress and pipe geometry as under tested conditions. The d_i evaluated using FE analysis and A-16 procedure has been compared.

Paris constants were generated as per the procedure given in ASTM E647 using three point bend (TPB) specimens machined from the pipe material which was fatigue tested. Hence, fatigue crack growth (FCG) life has been evaluated using these Paris constants. The ASME Boiler and Pressure Vessel Code Section XI also provides fatigue crack growth rate curves for carbon steel material under air environment based on small specimens. In this paper, a comparison has been made amongst the experimentally obtained fatigue crack growth curve (*a* versus *N*) and two analytical growth curves whose Paris constants were derived from two different sources which are experiments conducted on the specimens & the ASME Section XI.

3 EXPERIMENTAL DETAILS

3.1 Piping material

All the tests were carried out on seamless pipes made of SA 333 Gr. 6 carbon steel material used in Indian PHWRs. The pipes were in normalized and tempered condition and conform to the specifications of ASME Section II and Section III. The chemical composition and tensile properties of the material are as tabulated in Table 1 and 2.

Table 1. Chemical composition (in wt%) of pipe material

C	Mn	Si	P	S	Al	Cr	Ni	V	N
0.14	0.9	0.25	0.016	0.018	<0.1	0.08	0.05	<0.01	0.01

Table 2. Tensile properties at room temperature

Yield strength σ_y (MPa)	Ultimate tensile strength σ_u (MPa)	Elongation (%)	Percentage reduction in area
302	450	36.7	72.96

Cyclic stress–strain and low cycle fatigue properties have been obtained following ASTM E606 using smooth specimens of 4.5 mm gauge diameter machined from the same pipe material. Tests have been conducted under fully reversible condition for different strain ranges at room temperature and air environment. The cyclic stress–strain curve is given by eqn (1). The various constants in the equation have been obtained by fitting the test data points of the experiments.

$$\Delta \varepsilon /2 = 100\ (\Delta\sigma/2E) + (\Delta\sigma/2k)^{1/n} \quad (1)$$

k=354.27MPa n = 0.1523

The fatigue life curve is given by Basquin-Manson fit as shown in eqn (2),

$$\frac{\Delta\varepsilon}{2} = 100\frac{\sigma_f'}{E}(2N_i)^b + \varepsilon_f'(2N_i)^c \quad (2)$$

σ_f' = 586.06 MPa, b = -0.0757,

ε_f' = 24.06 %, c = -0.4814, E= 203 GPa

where, N_i is the number of cycles required for complete failure of the specimen and $\Delta\varepsilon/2$ is the total strain amplitude in percentage (%).

A set of fatigue crack growth rate experiments were conducted on TPB specimens (machined from the same piping material) using ASTM E647. The material constants have been evaluated after fitting the test data points in the form of Paris Law as given by eqn (3) below,

$$\frac{da}{dN} = C(\Delta K)^m \qquad (3)$$

where, C = 3.982 x 10^{-12} and m = 3.01

*d*a/*d*N is the crack growth rate in m/cycle, whereas ΔK is in $MPa\sqrt{m}$.

3.2 Test set up and procedure

The test set up schematic has been shown in Fig. 1(a). It consists of servo-hydraulic loading arrangement of $\pm 1000kN$ and $\pm 50mm$ actuator displacement capacity. The support system consists of two rollers at 2500mm apart and inner rollers on loading side, are separated by 880mm. This type of loading simulates pure bending in the inner span of test specimen.

The gauges working on the principle of Alternating Current Potential Drop (ACPD) technique have been used for observing the crack growth with number of cycles, during fatigue crack growth (FCG) test. The ACPD technique had an accuracy to measure the crack growth of 0.1mm. Hence, the crack growth of 0.1mm at the deepest point is set as the initiation life criterion. These gauges have been connected all along the length of the notch to obtain the evolving crack front with loading cycles.

3.3 Test Conditions

All the six tests have been carried out at room temperature and air environment under load controlled conditions with sinusoidal waveform of loading. The loading frequency was kept within the range of 0.5Hz to 1Hz. The outer diameter of all the pipes is 219mm. The loading and notch geometrical details are given in Table 3.

Table3. Details of loading, notch dimensions & cycles for fatigue crack initiation (N_i)

Specimen	**t (mm)**	**2C (mm)**	**a (mm)**	**r (mm)**	**Z (mm)**	**L (mm)**	**P_{max} (*k*N)**	**R**	**N_i (Test data)**
PBSC-8-1	15.58	114.3	2.01	0.1	2500	880	170	0.1	53000
PBSC-8-2	15.38	113.4	1.97	0.1	2500	880	250	0.5	320000
PBSC-8-3	15.12	110.0	3.00	0.1	2500	880	160,200	0.5	177000,58000
PBSC-8-4	15.38	113.0	3.50	0.1	2500	880	160	0.1	6000
PBSC-8-5	15.17	113.8	5.98	0.1	2500	880	165,175	0.5	32000,13000
PBSC-8-6	15.13	113.2	5.50	0.1	2500	880	150	0.1	3000

t-thickness of pipe, 2C-notch length, a-notch depth, r-notch root radius, Z-outer span, L-inner span, P_{max}-maximum load to the actuator, R-load ratio, N_i- initiation life corresponding to first 0.1mm crack growth.

It is to be noted from Table 3 that PBSC-8-3 and PBSC-8-5 have been subjected to block loading till initiation event. For example, PBSC-8-3 was first subjected to maximum load of 160 kN for 177000 cycles and the crack initiation event was observed in 58000 more cycles under increased maximum load of 200kN. The notch schematic is shown in Fig. 1(b).

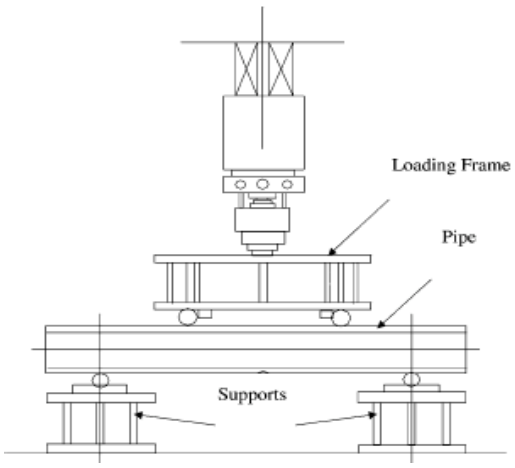

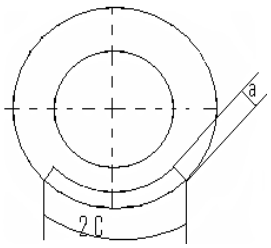

Figure 1(a) Test set up for pipe

Figure 1(b) pipe cross section at notch plane

4 FATIGUE CRACK INITIATION STUDY

Analyses were performed for these tests to predict crack initiation life using A-16 guide of RCC-MR which provides a procedure based on the pseudo elastic principal stress range ($\Delta\sigma_1$) in the proximity of notch root. The $\Delta\sigma_1$ ahead of notch root is generally evaluated using Creager's formulae. Further, the effective elastic strain range is evaluated based on equivalent uniaxial $\Delta\sigma_1$ stress range. The elastic-plastic local strain range amplification is made using Neuber's hyperbola followed by the plastic strain correction (Moulin and Roche (1985)) to account for effective poisson's ratio as given by Henky's flow rule for proportional loading.

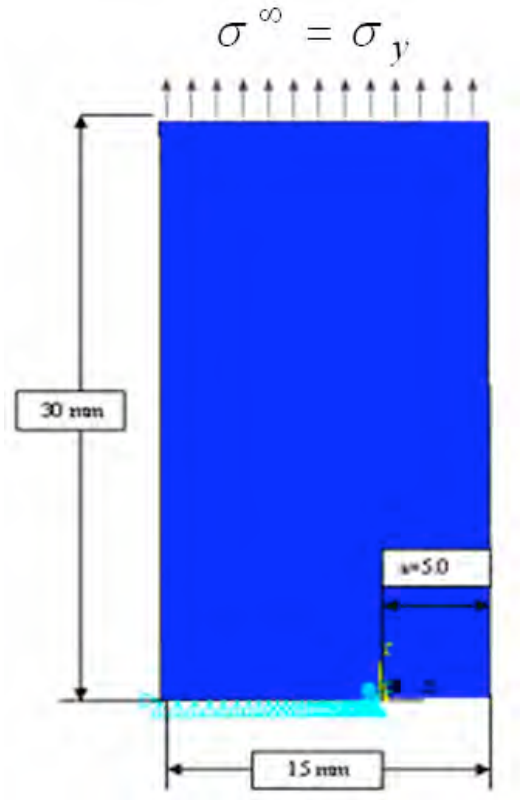

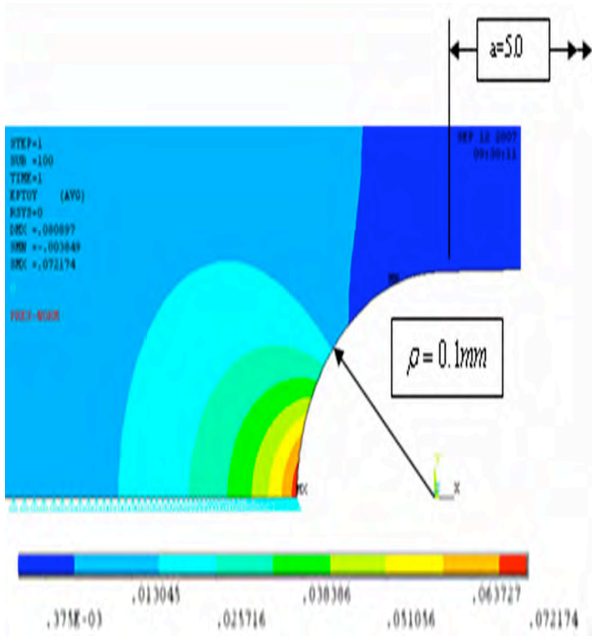

Figure 2(a) Typical geometry loaded with uniform traction **Figure 2(b)** typical strain contours near notch

A16 requires calculations to be carried out at characteristic distance (d_i) from the notch root which is stated to be a material specific parameter by A-16 irrespective of the load applied and notch dimensions. The characteristic distance (d_i) was back calculated from uniaxial fatigue failure curve (that is eqn 2) using experimentally found number of cycles for crack initiation and is evaluated to be 55μm and 100μm for two tests whereas rest four tests show d_i to be nearly 70μm.

In absence of body forces, plane stress and plane strain solutions give identical stress states and hence A-16 procedure will lead to same fatigue initiation life. However, it is known that the strain ranges will be different for the two cases and so as the fatigue lives. Hence, effective stress and effective strain ranges, both should be evaluated from the actual state of stress and strain at the notch tip. In view of this, two dimensional finite element parametric study is carried out with different crack depth to specimen width ratios (a/W) for plane stress and plane strain conditions to see the effects of the state of stress/ strain on initiation life. Eight node quadrilateral elements were used to discretize plane two dimensional geometry. The typical two dimensional geometrical model and strain contours are shown in Fig. 2. The typical strain amplitudes as obtained from finite element analysis and A-16 procedure are compared in Fig. 3 for plane stress and plane strain cases. It can be concluded that A-16 procedure predicts the initiation life with reasonable accuracy for plane strain geometrical condition, whereas it over predicts the initiation life for plane stress case.

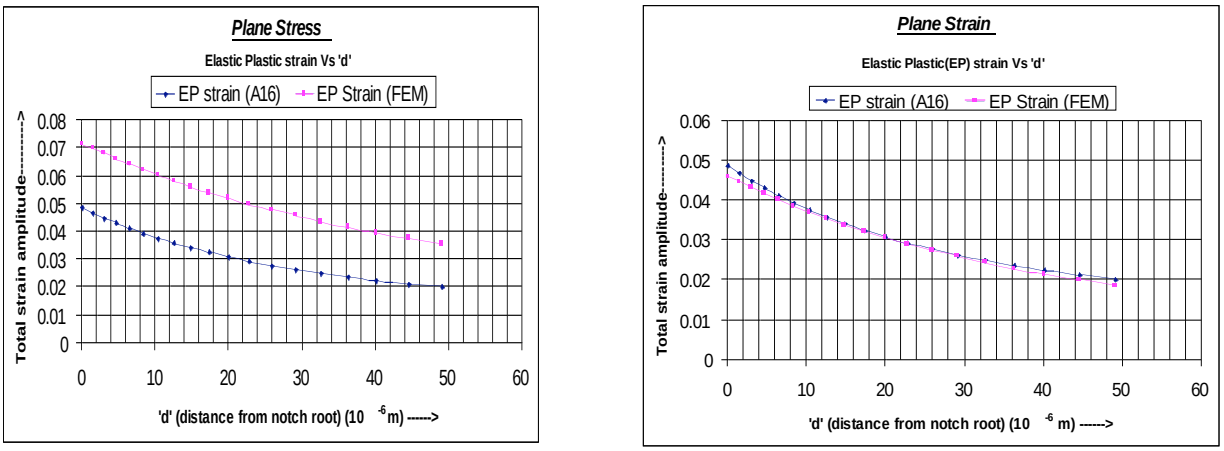

(a) (b)

Figure 3. Variation of elastic-plastic strain amplitude as obtained from 2D FE analysis and A16 procedure with distance from notch root for **(a)** Plane stress, **(b)** Plane strain geometry

However, the actual pipe cases where geometry also plays a major role can neither be attributed as completely plane strain nor plane stress as prescribed in the Creager's formulae. It may be lying somewhere in between the two extreme cases. Therefore, detailed elastic plastic finite element analyses have been carried out for actual pipes under as tested conditions. One quarter domain of the test specimen was modeled using 20 noded 3D brick elements, with the finest mesh size of 20 μm near the point of singularity. The stabilized cyclic stress strain data for SA-333 Gr. 6 was used for the analysis (that is eqn 1). The LCF tests were conducted under uniaxial and completely reversible loading conditions. Hence, correction factors for mean stress (Morrow(1968)) and multiaxiality (Manson & Halford (1977)) have been accounted in the uniaxial $\Delta\varepsilon - N$ curve. The corrected fatigue failure curve is as given by eqn (4),

$$(\%)\frac{\Delta\varepsilon}{2} = 100\frac{(\sigma_f'(M.F.)^n - \sigma_m)}{E}(2N_i)^b + \varepsilon_f'(M.F.)(2N_i)^c \qquad (4)$$

where, σ_f' = 586.06 MPa, b = -0.0757, ε_f' = 24.06 %, c = -0.4814, n = 0.1523

σ_m = mean stress (MPa)

$$M.F. = e^{-0.5(TF-1)} \quad ; \text{if } TF \geq 1.0 \qquad (5)$$

$$= 1.0 \quad ; \text{if } TF < 1.0$$

Triaxiality Factor (TF) = σ_h / σ_{eff}

$$= \sqrt{2}\,(\sigma_1+\sigma_2+\sigma_3)/\{3[(\sigma_1-\sigma_2)^2 + (\sigma_2-\sigma_3)^2 + (\sigma_3-\sigma_1)^2]^{1/2}\} \qquad (6)$$

σ_h = hydrostatic stress = $(\sigma_1+\sigma_2+\sigma_3)/3$

σ_{eff} = effective stress (or von-mises stress)

$= (1.0/\sqrt{2})[\ (\sigma_1-\sigma_2)^2 + (\sigma_2-\sigma_3)^2 + (\sigma_3-\sigma_1)^2\ ]^{1/2}$

σ_1, σ_2, σ_3 = Three Principal Stresses

Here, eqn (4) is the modified version of Basquin- Manson fit as given in eqn (2). It is well understood that the higher constraint reduces the ductility of the material. Therefore, an artificial penalty is imposed in the plastic strain part of the fatigue life curve to take care of the reduction in ductility.

Table4. Comparison of characteristic distance as calculated from A-16 and 3D FE analysis.

Specimen	a/t	2C/a	P_{max} (kN)	R	N_i (Test data)	Characteristic distance d_i (µm)	
						A-16	FEA
PBSC-8-1	0.13	57	170	0.1	53000	70	36
PBSC-8-2	0.13	58	250	0.5	320000	68	68
PBSC-8-3	0.20	37	160,200	0.5	177000,58000	70	57
PBSC-8-4	0.23	32	160	0.1	6000	55	40
PBSC-8-5	0.39	19	165,175	0.5	32000,13000	100	88
PBSC-8-6	0.36	21	150	0.1	3000	75	62

Thus, the number of cycles to crack initiation (N_i) can be calculated from corrected fatigue-failure curve using elastic-plastic strain amplitude as obtained from FE analysis at different 'd' distances from notch root. The distance at which the number of cycles corresponding to effective elastic plastic strain amplitude matches with the experimental value, is taken as 'characteristic distance(d_i)'. The characteristic distance is found to be varying between 36µm to 88 µm as shown in Table 4.

Further, the definition of 'd_i' has been analyzed in the context of some damage parameters like tri-axiality factor (T.F.) in conjunction with plastic strain range ($\Delta\varepsilon_p$) at a distance from notch tip. The higher constraint in the form of T.F. suppresses the plasticity. The typical variations of T.F. and $\Delta\varepsilon_p$ with distance from the root, are as plotted in Fig. 4. It can be observed that T.F. is maximum at around 100µm and the total equivalent plastic strain range almost vanishes at such distance. The results point to a critical / characteristic distance from the notch root where the material sees maximum damage and causes crack initiation. The variation of T.F. and $\Delta\varepsilon_p$ depend upon load applied, notch geometrical parameters etc. Therefore, it is difficult to comment d_i to be a material specific and treat variation in d_i as observed. However, this argument is based on the tests conducted till date on this material.

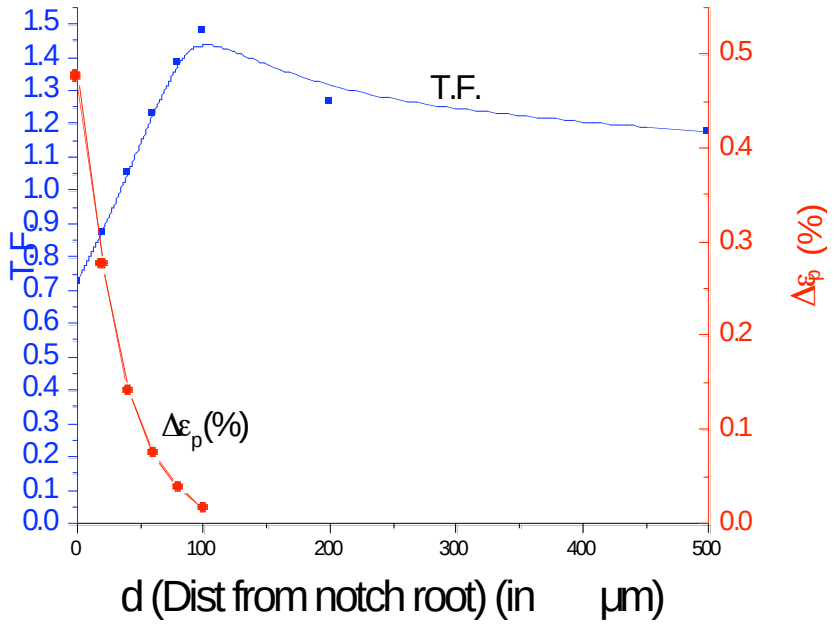

Figure 4. FEA results: Typical variation of TF and % $\Delta\varepsilon_p$

5 FATIGUE CRACK GROWTH

Once the crack has initiated, the pipes were continued to be tested till the crack becomes through wall. The crack growth at different locations all along the notch length was recorded with number of cycles using ACPD technique.

The FCG analytical study is carried out following Paris Law with two sets of material growth constants. One set of Paris constants has been derived from the FCGR tests conducted on TPB specimens (eqn 3), whereas the second set of constants have been obtained from ASME Sec XI for air environment. The experimental FCG data are found to be in reasonably close agreement with the analytical results for the first set of material growth constants (Fig. 5).

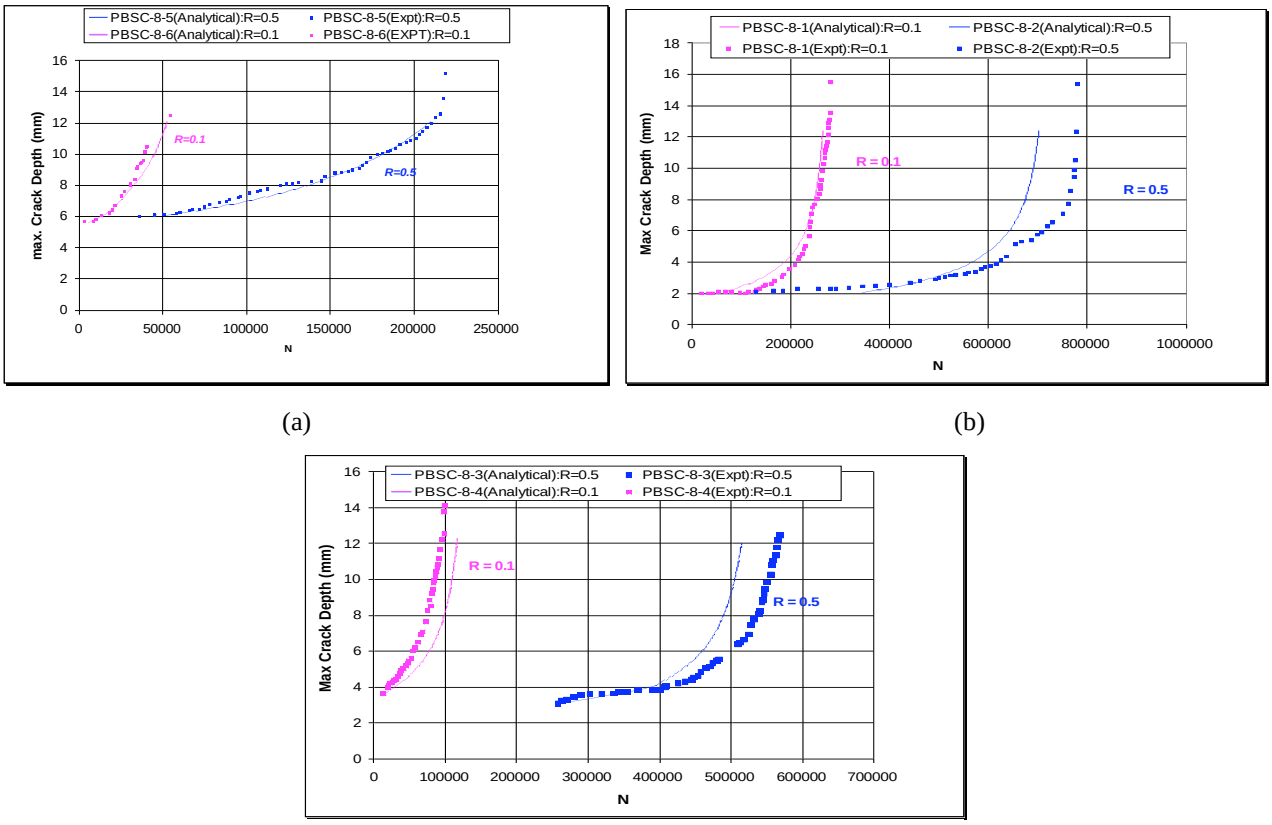

Figure 5. Comparison of FCG test data of maximum crack depth with Paris Law governed crack growth using Paris constants derived from TPB specimens

Similarly, the analytical maximum crack depth has been evaluated with respect to number of cycles using second set of Paris constants show the conservatism of ASME over experimental data (Fig. 6).

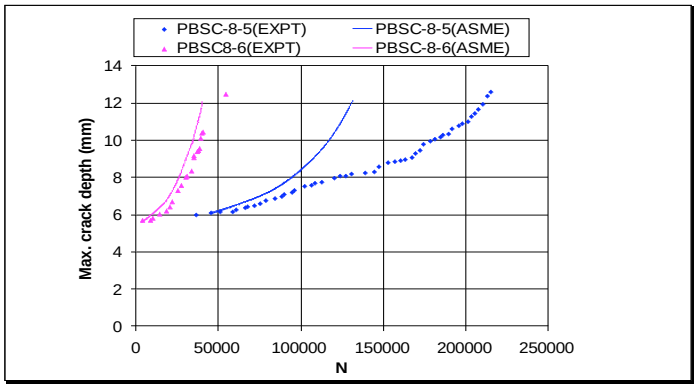

Figure 6. Comparison of FCG test data of maximum crack depth with Paris Law governed crack growth using Paris constants as obtained from ASME Section XI

6 CONCLUSION

The experimental, analytical and FE studies carried out on the CS pipes of outer diameter 219mm and 15.1 mm thickness conclude the followings for fatigue crack initiation and growth.

6.1 Fatigue Crack initiation

(a) A-16 procedure predicts the initiation life quite accurately for plane strain geometry, whereas it over predicts the life for plane stress condition.

(b) Characteristic distance (d_i) as calculated from A-16 and three dimensional finite element analysis, is found to have significant variation. The d_i is further analyzed considering the damage caused by higher constraint effect and plastic strain and concluded to be load and notch dimensions dependent parameter. However, this argument is based on the 6 tests conducted on CS pipes.

6.2 Fatigue crack growth

The experimental growth data is in good agreement with analytical crack growth as governed by Paris law for the material growth constants derived from standard TPB specimens machined from the same piping material. The fatigue crack growth curve as specified in ASME Section XI produces conservative results.

REFERENCES

Singh P.K., Vaze K.K., Bhasin V., Kushwaha H.S., Gandhi P., Ramachandra Murthy D.S., Crack initiation and growth behavior of circumferentially cracked pipes under cyclic and monotonic loading. Int J Pressure Vessel Piping 80(2003) 629-640.

Neuber, H., "Theory of stress concentration for shear-strained prismatical bodies with arbitrary non-linear stress strain law," Journal of Applied Mechanics, Transactions of ASME, Vol. 28, Dec. 1961; pp. 544-550.

Topper, T.H., Wetzel, R.M. and Morrow, J., "Neuber's rule applied to fatigue of notched specimens," Journal of Materials, Vol. 4, No.1, March 1969, pp. 200-209.

Hoffmann M., Seeger T., A generalized method for estimating multiaxial elastic plastic notch stresses and strains. Transactions of ASME, vol-107/1985, pp 250-260.

Molski K, Glinka G. A method for elastic–plastic stress and strain calculation at a notch root. Mater Sci Eng 1981;50(1):93-100.

A16 guide of RCC-MR for defect assessment and leak before break analysis. Edition 2002.

E647-93, Standard test method for measurement of fatigue crack growth rate. Annual book of ASTM standard, vol. 03.01.; 1995. pp. 569–96.

Rules for in-service inspection of nuclear power plant components. ASME Boiler and Pressure Vessel Code, Section XI, New York;2001.

E606-93, "A standard practice for strain controlled fatigue testing" Annual book of ASTM standards, vol. 03.01, 1995.

Moulin D., Roche R.L., Correction of the Poisson effect in the elastic analysis of Low-cycle fatigue, Int. J. Pres. Ves. & Piping 19 (1985), 213-233.

Manson S.S. & Halford G.R., (1977), Multiaxial low cycle fatigue of Type 304SS. Journal of Engineering Material Technology, pp 283-285.

Morrow J., Fatigue design handbook, Advances in engineering, vol. 4, Society of Automotive Engineers, Warrendale, Pa., 1968, sec. 3.2, pp 21-29.